

Substrate orientation effects on dopant incorporation in InP grown by metalorganic chemical vapor deposition

Paul R. Berger,^{a)} S. N. G. Chu, R. A. Logan, Erin Byrne, D. Coblenz, James Lee III, Nhan T. Ha, and N. K. Dutta
AT&T Bell Laboratories, Murray Hill, New Jersey 07974

(Received 31 August 1992; accepted for publication 6 January 1993)

We have investigated the doping incorporation and activation of InP growth using metalorganic chemical vapor deposition on $\langle 100 \rangle$, $\langle 311 \rangle$ B, and $\langle 110 \rangle$ InP substrates. Effects of orientation, growth temperature, and V/III fluxes were studied. The dopants used were Zn from dimethylzinc [(CH₃)₂Zn] and diethylzinc [(C₂H₅)₂Zn], S from hydrogen sulfide [H₂S], Si from silane [SiH₄], and Sn from tetraethyltin [(C₂H₅)₄Sn]. The incorporation and activation of the *p*-type dopant Zn are elevated on the $\langle 311 \rangle$ B and $\langle 110 \rangle$ planes, while the incorporation is suppressed for the *n*-type dopants (S, Si, and Sn). The *n*-type dopant Sn has similar incorporation and activation on the various substrate orientations studied. Anomalous Zn doping on the higher order planes $\langle 311 \rangle$ B and $\langle 110 \rangle$ lead to the Zn incorporation exceeding the solubility limit in InP. Incorporated Zn levels as high as $1.0 \times 10^{19} \text{ cm}^{-3}$ were measured, and the corresponding activated Zn level was as high as $5.4 \times 10^{18} \text{ cm}^{-3}$ on a $\langle 110 \rangle$ InP substrate. Interdiffusion of the *p*-type dopant Zn into the S-doped *n*-type InP substrate is inhibited by a high S-doping level and segregates at the substrate–epilayer interface. If the S-doping level is lower than the Zn concentration, then Zn diffuses deep into the substrate at a uniform level.

Anomalous doping behavior on higher order planes has been seen in GaAs grown by molecular beam epitaxy.^{1,2} Si-doped GaAs which is *n*-type on (100) substrates, becomes *p*-type on (111)A planes. The type conversion is mainly explained by the amphoteric behavior of Si residing on As sites rather than Ga sites. Deep levels are also shown to cause significant compensation.

GaAs lasers have been realized which employ this plane-dependent doping on patterned substrates.^{3–5} By taking advantage of the plane-selective doping mechanism of amphoteric dopants, a lateral *p–n* junction can be formed on a *v*-groove etched substrate when it is overgrown. This effectively lowers the threshold current by creating low leakage blocking layers. Marclay *et al.*⁵ have achieved sub-milliamper threshold current using this technique.

Doping in metalorganic chemical vapor deposition (MOCVD) grown InP has been studied on (100) substrates from dimethylzinc⁶ [(CH₃)₂Zn], S from hydrogen sulfide⁷ [H₂S], Si from silane⁸ [SiH₄], and Sn from tetraethyltin⁹ [(C₂H₅)₄Sn]. However, the behavior of dopant incorporation on other crystal planes has not been studied. In this communication, we investigate the effects of substrate orientation, growth temperature, and V/III flux ratio on the incorporation of Zn, S, Si, and Sn in InP grown on $\langle 100 \rangle$, $\langle 311 \rangle$ B, and $\langle 110 \rangle$ substrates.

Bulk layers of InP were grown by MOCVD on $\langle 100 \rangle$, $\langle 311 \rangle$ B, and $\langle 110 \rangle$ InP substrates mounted side-by-side on the same susceptor. The layers studied were grown in both low pressure (100 mbar) and atmospheric MOCVD reactors (both horizontal) which utilize the group III precursors trimethylindium and trimethylgallium, and group V hydrides phosphine (PH₃) and arsine (AsH₃). The

sources for the dopants were hydrogen sulfide (S), silane (Si), tetraethyltin (Sn), and dimethylzinc at low pressure and diethylzinc at atmospheric pressure (Zn). The layers were typically doped to about $1\text{--}3 \times 10^{18} \text{ cm}^{-3}$ for the $\langle 100 \rangle$ orientation. No semi-insulating material was grown or studied. The temperature profile of the susceptor used has been determined to be uniform and only small samples ($\sim 1 \text{ cm}^2$) were grown and studied. The doping was measured by electrochemical *C–V* profiling (Polaron) and secondary ion mass spectroscopy (SIMS). Polaron measures the active dopant level, while SIMS measures the total amount incorporated regardless of its electrical activity. A ratio of both values gives a good estimate of the activation percentage.

The first set of bulk InP layers grown on $\langle 100 \rangle$, $\langle 311 \rangle$ B, and $\langle 110 \rangle$ InP substrates were nominally doped with *n*-type dopants (i.e., S, Si, and Sn). As shown in Table I, the dopant incorporation on the $\langle 100 \rangle$ substrate as measured by SIMS was $\sim 1\text{--}3 \times 10^{18} \text{ cm}^{-3}$. Polaron measured an activation of $\sim 92\%$ – 94% for the S-doped, Si-doped, and Sn-doped InP layers. However, on the $\langle 311 \rangle$ B substrate, the S incorporated an order of magnitude less as compared to the $\langle 100 \rangle$ substrate, and only 65% was activated. The Si-doped and Sn-doped InP had about the same dopant incorporation on the $\langle 311 \rangle$ B substrate as compared to the $\langle 100 \rangle$ plane, but 82%–86% was activated. On the $\langle 110 \rangle$ InP substrate, the S-doped layer again had an order of magnitude lower dopant incorporation than the $\langle 100 \rangle$ plane, and the measured active doping level showed almost unity activation. The Si-doped wafer on the $\langle 110 \rangle$ InP substrate also had a reduced dopant incorporation, even lower than the Si incorporation on the $\langle 311 \rangle$ B substrate, but the activation percentage dropped only slightly as compared to $\langle 100 \rangle$ orientation. The most reliable *n*-type dopant studied was the Sn-doped layers, which had similar

^{a)}Present address: University of Delaware, Newark, DE 19716.

TABLE I. Dopant incorporation and activation in atmospheric (S and first Zn data point) and low-pressure (Si, Sn, and second Zn data point) MOCVD-grown doped InP.

Layer	$\langle 100 \rangle$		$\langle 311 \rangle B$		$\langle 110 \rangle$	
	Polaron (%) ^a	SIMS	Polaron (%) ^a	SIMS	Polaron (%) ^a	SIMS
Sulfur	2.4×10^{18} (92%)	2.6×10^{18}	7.1×10^{16} (65%)	1.1×10^{17}	1.8×10^{17} (99%)	1.82×10^{17}
Silicon	9.0×10^{17} (94%)	9.6×10^{17}	8.8×10^{17} (82%)	1.1×10^{18}	3.2×10^{17} (86%)	3.7×10^{17}
Tin	2.7×10^{18} (94%)	2.9×10^{18}	2.2×10^{18} (86%)	2.6×10^{18}	2.6×10^{18} (96%)	2.7×10^{18}
Zinc	1.8×10^{18} (64%)	2.8×10^{18}	5.1×10^{18} (91%)	5.6×10^{18}	5.0×10^{18} (56%)	8.9×10^{18}
Zinc	1.9×10^{18} (94%)	2.0×10^{18}	3.1×10^{18} (55%)	5.7×10^{18}	3.2×10^{18} (75%)	4.3×10^{18}

^aPercent activation (Polaron/SIMS).

dopant incorporation and activation levels with only slight fluctuation from 86% to 96%, regardless of the substrate orientation. Doping with Sn on patterned substrates, therefore, could be very predictable over a step edge.

A second set of bulk InP layers were also grown on $\langle 100 \rangle$, $\langle 311 \rangle B$, and $\langle 110 \rangle$ InP substrates using dimethylzinc and diethylzinc from which Zn acts as a *p*-type dopant. Samples were grown in two separate MOCVD reactors (low-pressure and atmospheric) and yielded slightly different results. In both cases, the dopant incorporation was significantly elevated on the higher order planes ($\langle 311 \rangle B$ and $\langle 110 \rangle$), but the amount of elevation varied in both reactors as well as the compensation levels. On the $\langle 110 \rangle$ InP substrate, an incorporated Zn level of $8.9 \times 10^{18} \text{ cm}^{-3}$ was measured which is above the solubility limit for InP.^{6,10} Morphology of all layers was good. This result has been repeated. Previous studies of MOCVD⁶ and liquid phase epitaxy (LPE)¹⁰ report that Zn levels saturate in InP $\sim 3 \times 10^{18} \text{ cm}^{-3}$ active level ($N_A - N_D$). The effects of other growth parameters on the Zn doping were then investigated to further study this anomalous doping behavior.

More Zn-doped InP samples were grown using two different commercial MOCVD reactors and varying the growth temperature and III/V ratio on $\langle 100 \rangle$ and $\langle 110 \rangle$ InP substrates. Again, both orientations are grown simultaneously. The nominal doping level aimed for was $\sim 2 \times 10^{18} \text{ cm}^{-3}$ on the $\langle 100 \rangle$ substrate. The results of the Zn-doped InP with varying growth conditions are shown in Table II. Figure 1 shows the dopant concentration on an Arrhenius plot. In both reactors, the effect of substrate temperature was consistent, the level of active and incor-

porated Zn-doping decreased with increasing substrate temperature. The same doping dependence on substrate temperature was found by Glew¹¹ for Zn-doped GaAs grown by organometallic vapor phase epitaxy (OMVPE). This could be caused by the reevaporation of Zn from the surface at elevated temperatures, or the increased compensation of Zn residing on P sites rather than In sites at the higher doping levels. The incorporated and activated Zn levels linearly increased with decreased temperature on the $\langle 100 \rangle$ InP substrate, but also became more compensated. This is supported by Wada *et al.*¹⁰ who speculate that increased compensation at higher Zn doping accounts for the saturation of Zn-doping. However, on the $\langle 110 \rangle$ InP substrate the active and incorporated Zn-doping increased linearly with reduced temperature without any change in the compensation levels. Thus, Zn-doping levels above $3 \times 10^{18} \text{ cm}^{-3}$ which has been the established saturation or solubility limit^{6,10,11} were measured. The highest Zn level measured by SIMS was $1.0 \times 10^{19} \text{ cm}^{-3}$ on a $\langle 110 \rangle$ substrate grown at 575 °C. The corresponding Polaron level ($N_A - N_D$) was $5.4 \times 10^{18} \text{ cm}^{-3}$ on the same $\langle 110 \rangle$ InP substrate. The effect of increased overpressure of phosphine was an elevated Zn incorporation by nearly 50%, but the activation level dropped by the same amount which resulted in identical activated Zn levels as measured by Polaron on both sets of samples.

Diffusion of Zn was also investigated. Zn starts to diffuse into the S-doped substrate when the Zn-doping level is high. The diffusion profile varies with the adjacent substrate S-doping level. If the Zn level is lower than the S-doping, then Zn tends to segregate at the substrate-epilayer interface. However, if the Zn level is elevated

TABLE II. Dopant incorporation and activation in atmospheric (first three data points) and low-pressure (last four data points) MOCVD-grown Zn-doped InP.

Layer	$\langle 100 \rangle$		$\langle 110 \rangle$	
	Polaron (%) ^a	SIMS	Polaron (%) ^a	SIMS
575 °C	2.6×10^{18} (53%)	4.9×10^{18}	5.4×10^{18} (54%)	1.0×10^{19}
625 °C	1.8×10^{18} (65%)	2.8×10^{18}	4.6×10^{18} (53%)	8.7×10^{18}
675 °C	1.1×10^{18} (78%)	1.4×10^{18}	3.4×10^{18} (55%)	6.2×10^{18}
600 °C V/III=1	1.5×10^{18} (52%)	2.3×10^{18}	3.3×10^{18} (40%)	7.2×10^{18}
660 °C V/III=1	1.2×10^{18} (52%)	2.3×10^{18}	2.9×10^{18} (55%)	5.3×10^{18}
660 °C V/III=2	1.2×10^{18} (45%)	3.3×10^{18}	2.9×10^{18} (37%)	8.7×10^{18}
700 °C V/III=1	9.0×10^{17} (68%)	1.3×10^{18}	2.4×10^{18} (53%)	4.5×10^{18}

^aPercent activation (polaron/SIMS).

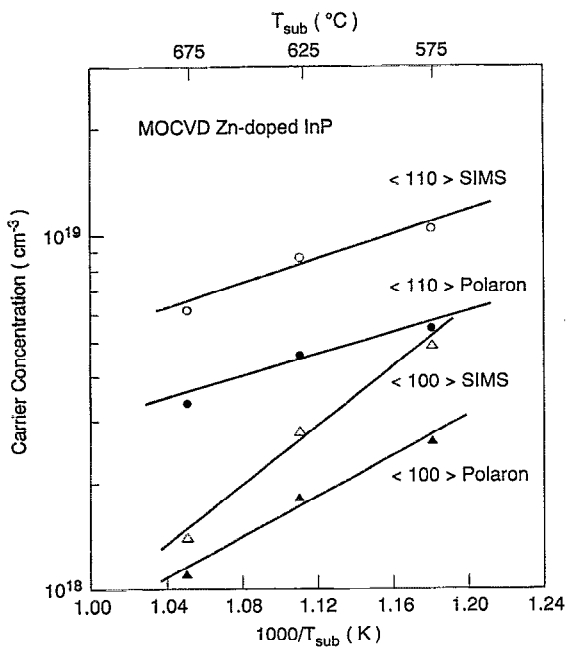


FIG. 1. Arrhenius plot of Zn-dopant incorporation and activation as measured by SIMS and polaron for atmospheric MOCVD InP growth on $\langle 100 \rangle$ and $\langle 110 \rangle$ InP substrates.

above the S-doping, then Zn diffuses into the substrate at a constant level. The higher the Zn level in the epilayer the deeper the Zn diffuses into the substrate. This same phenomenon has also been observed in Zn/Si-doped interfaces.¹² The results of Zn segregation at the interface is shown in Fig. 2(a) with a S-doping level of $4.0 \times 10^{18} \text{ cm}^{-3}$ and the Zn-doping level is also $\sim 4.0 \times 10^{18} \text{ cm}^{-3}$. In Fig. 2(b), where the S-doping level is $4.0 \times 10^{17} \text{ cm}^{-3}$, much lower than the Zn-doping level of $\sim 9.0 \times 10^{18} \text{ cm}^{-3}$, the Zn diffuses deep into the substrate.

In conclusion, of the n -type dopants measured, Sn is the most consistent dopant in InP on different InP substrate orientations. Si and S dopants yielded much lower active dopant levels on $\langle 311 \rangle$ B and $\langle 110 \rangle$ InP planes than on the $\langle 100 \rangle$ plane. The p -type dopant investigated was Zn and showed an anomalous behavior. Unlike the n -type dopants, Zn had an enhanced dopant incorporation. Levels of Zn measured were higher on the $\langle 110 \rangle$ InP surface than the previously reported solubility limit. Activated Zn levels were measured as high as $5.4 \times 10^{18} \text{ cm}^{-3}$ on a $\langle 110 \rangle$ InP substrate.

The authors would like to thank R. Karlicek for useful discussions, and Judy Grenko for MOCVD assistance (AIX).

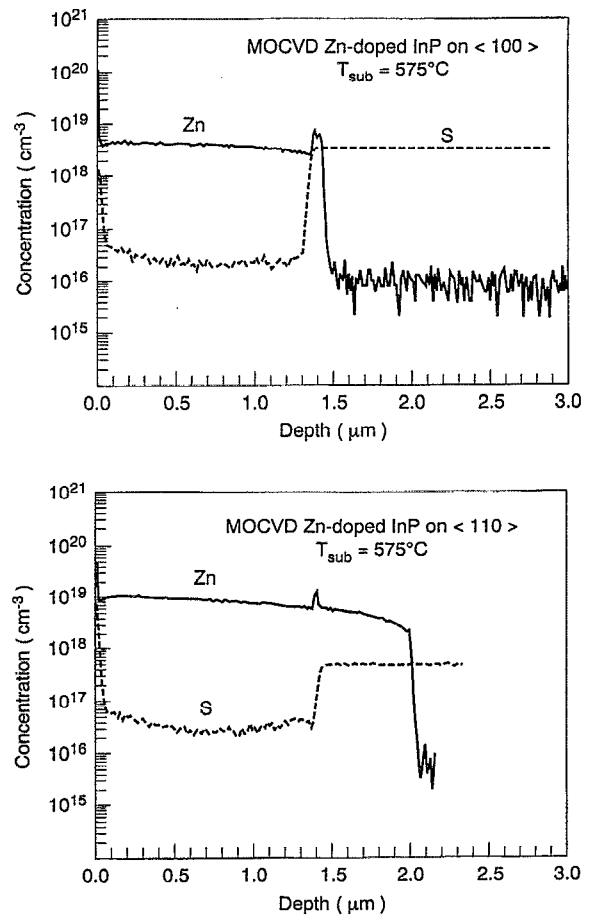


FIG. 2. (a) SIMS data of Zn segregation at substrate for S-doping level of $4.0 \times 10^{18} \text{ cm}^{-3}$, and (b) SIMS data of Zn interdiffusion into InP substrate at a substrate doping level of $4.0 \times 10^{17} \text{ cm}^{-3}$ for atmospheric MOCVD InP growth.

- ¹J. M. Ballingall and C. E. C. Wood, *Appl. Phys. Lett.* **41**, 947 (1982).
- ²D. L. Miller, *Appl. Phys. Lett.* **47**, 1309 (1985).
- ³H. P. Meier, R. F. Broom, P. W. Epperlein, E. van Geison, Ch. Harder, H. Jäckel, W. Walter, and D. J. Webb, *J. Vac. Sci. Technol. B* **6**, 692 (1988).
- ⁴H. Jäckel, H. P. Meier, G. L. Bona, W. Walter, D. J. Webb, and E. Van Gieson, *Appl. Phys. Lett.* **55**, 1059 (1989).
- ⁵E. Marclay, D. J. Arent, C. Harder, H. P. Meier, W. Walter, and D. J. Webb, *Electron. Lett.* **25**, 892 (1989).
- ⁶A. W. Nelson and L. D. Westbrook, *J. Appl. Phys.* **55**, 3103 (1984).
- ⁷R. Logan, T. Tanbun-Ek, and A. M. Sargent, *J. Appl. Phys.* **65**, 3723 (1989).
- ⁸A. R. Clawson, T. T. Vu, and D. I. Elder, *J. Cryst. Growth* **83**, 211 (1987).
- ⁹C. J. Pinzone, N. D. Gerrard, R. D. Dupuis, N. T. Ha, and H. S. Luftman, *Electron. Lett.* **25**, 1315 (1989).
- ¹⁰O. Wada, A. Majerfeld, and P. N. Robson, *J. Electrochem. Soc.* **127**, 2278 (1980).
- ¹¹R. W. Glew, *J. Cryst. Growth* **68**, 44 (1984).
- ¹²C. Blaauw, F. R. Shephard, and D. Eger, *J. Appl. Phys.* **66**, 605 (1989).